Polyphenols Deriving from Chalcones: Investigations of Redox Activities

Nicole Cotelle,*,† Philippe Hapiot,*,‡ Jean Pinson,§ Christian Rolando,† and Hervé Vézin†

Laboratoire de Chimie Organique et Macromoléculaire, UMR CNRS−Université des Sciences et Technologies de Lille, N 8009, F-59655 Villeneuve d'Ascq Cedex, France, Laboratoire d'Electrochimie Moléculaire et Macromoléculaire, SESO, UMR CNRS−Institut de Chimie de Rennes, Campus de Beaulieu, N 6510, F-35042 Rennes, France, and Alchimer, 15 rue du Buisson aux Fraises, F-91300 Massy, France

The redox properties of a series of hydroxychalcones (a group of polyphenols abundantly present in plants) were investigated by cyclic voltammetry. As for many polyphenols, their beneficial properties have been mainly related to their antioxidant activities, which in turn are directly associated to their redox behavior. Two types of radicals can be produced that are localized on either one of the two aromatic systems. Their thermodynamic and kinetic parameters were extracted and compared to the predictions of density functional theory calculations. When at least one OH is present on each ring, their behaviors are dominated by the conjugated system: phenolic ring A−double bond−ketone, which is the only one to be oxidized. However, the redox properties of this conjugated system are strongly influenced by the presence of ring B. When an OH is present on ring B, an important feature is the existence of strong hydrogen bonding that remains almost unmodified even when ring A is oxidized. It does not considerably change the thermodynamics of ring A but strongly increases the rigidity of the molecule that remains planar under the neutral, anionic, or radical forms. Oxidation potentials of the phenolates range between 0.1 and 0.2 V versus a saturated calomel electrode, which correspond to species that are very easy to oxidize and lead to the rapid formation of nonradical species, underlining the potential antioxidant properties of these molecules.

Introduction

Hydroxychalcones are a group of polyphenols abundantly present in plants.[1,2] These compounds contain two aromatic rings (either phenyl or phenol groups) that are linked through an unsaturated side chain. In the nomenclature, these rings are classically reported as rings A and B (Chart 1). Many biological activities have been attributed to this group of molecules, such as anticancer,[3,4] antiinflammatory, antipyretic and analgesic,[3] cytotoxic in vitro,[5] bactericidal, insecticidal, antifungal,[3] antioxidant,[6] and phytoestrogenic activities.[7,8] Similar properties have been reported in synthetic chalcones. For example, preliminary studies indicate that some synthetic hydroxychalcones bearing *tert*-butyl groups on ring A present an in vitro antioxidant potential as proven by the prevention of oxidized low-density-lipoprotein-induced cytotoxicity.[9] Other examples of beneficial effects of synthetic flavonoids have been also reported on functional recovery after ischemia and reperfusion in isolated rat heart.[10] More generally, as is reported for other polyphenols, their beneficial properties have been mainly related to the antioxidant activities of the molecules.[11] However, as seen in the previous examples, though biological properties have been reported in numerous publications and are the subject of active research, their chemical-physics properties (redox potential, mechanism of formation and reactivities of generated radicals, selectivity of the different positions, etc.) are still waiting for
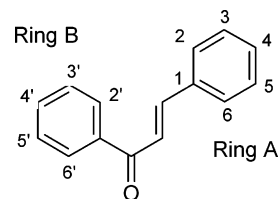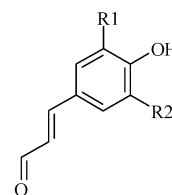
CHART 1

CHART 2

R1 = R2 = H coumaraldehyde
R1 = OCH₃, R2 =H coniferaldehyde
R1 =R2 = OCH3 sinapaldehyde

clear-cut answers and descriptions. Such knowledge is essential for understanding the processes in which the molecules are involved and consequently for the improvement or the design of synthetic analogues. In the case of polyphenols with several aromatic rings,[12] such as the polyhydroxychalcones, one of the first questions is clearly the identification and the characterization of the specific role of each ring and their mutual interactions. It is not surprising that several antioxidant properties are strongly related to the oxidation potential, pK_a, and reactivities of each ring. (See, for example, refs 12, 13, and 14 and references therein). To obtain more information in these fields,

* Author to whom correspondence should be addressed. Phone: (+33) (0) 2 23 23 59 39. Fax: (+33) (0) 2 23 23 62 92. E-mail: philippe.hapiot@ univ-rennes1.fr.
† Université des Sciences et Technologies de Lille.
‡ Université de Rennes 1.
§ Alchimer.

Phenols Deriving from Chalcones

J. Phys. Chem. B, Vol. 109, No. 49, 2005 **23721**

a series of hydroxychalcones were synthesized in which we varied the number and positions of OH groups on each ring. The redox behaviors were systematically investigated by cyclic voltammetry and analyzed to extract both the thermodynamic and the kinetic parameters.

Experimental Section

Chemicals: Synthesis of Hydroxychalcones. Chalcone derivatives were obtained by acid-catalyzed condensation of 3,5-dialkyl-4-hydroxybenzaldehyde and the corresponding acetophenone according to Claisen−Schmidt reactions in polar solvents according to the same general procedure published in ref 10 and references therein. They were purified by column chromatography. All solvents for synthesis were of commercial quality used from freshly opened containers and were dried and purified by conventional methods. Aryl methyl ketone and 3,5-dialkyl-4-hydroxybenzaldehydes were purchased from Aldrich-Chimie (St Quentin-Fallavier, France). Melting points were determined on a Reichert Thermopan apparatus, equipped with a microscope and are uncorrected. NMR spectra were obtained on a AC 300 Bruker spectrometer in DMSO-d_6 with tetramethylsilane as the internal reference. Mass spectra were recorded on a Thermo-Finnigan polarisQ mass spectrometer (70 eV, electronic impact). The X-ray diffractometric analysis of a representative compound (**9**) unambiguously confirms the E configuration of the double bond.

Syntheses and characterizations of 3-(4-hydroxy-3,5-dimethyl-phenyl)-1-phenyl-propenone (**1**), 1-(2-hydroxy-phenyl)-3-phenyl-propenone (**5**), 1-(4-benzyloxy-2-hydroxy-phenyl)-3-phenyl-propenone (**6**), and 3-(3,5-di-*tert*-butyl-4-hydroxy-phenyl)-1-(2-hydroxy-phenyl)-propenone (**9**) were previously published in refs 15, 16, 17, and 10, respectively.

1-(2-Benzyloxy-phenyl)-3-(4-hydroxy-3,5-dimethyl-phenyl)-propenone (2). Yield 70%, mp 134−135 °C. ^{1}H NMR ((CD$_3$)$_2$CO, 300 MHz): 2.15 (s, 6H, 2CH$_3$), 5.21 (s, 2H, CH$_2$), 7.07 (t, 1H, H-4′), 7.22 (s, 2H, H-2, H-6), 7.26−7.34 (m, 8H, H-arom, H-α), 7.46 (d, 1H, H-β, ^3J = 16 Hz), 7.51 (d, 1H, H-3′, ^3J = 7.44 Hz), 7.55 (d, 1H, ^3J = 7.3, H-6′), 8.89 (s, 1H, OH). M + 1 = 359.7.

1-(2,4-Bis-benzyloxy-phenyl)-3-(4-hydroxy-3,5-dimethyl-phenyl)-propenone (3). Yield 80%, mp 192 °C. ^{1}H NMR (DMSO-d_6, 300 MHz): 2.10 (s, 6H, 2CH$_3$), 3.35 (s, 1H, OH), 5.21 (s, 2H, CH$_2$), 5.22 (s, 2H, CH$_2$), 6.73 (dd, 1H, H-5′ ^3J = 8.64 Hz, ^4J = 2.09 Hz), 6.92 (d, 1H, ^4J = 2.09 Hz, H-3′), 7.15 (s, 2H, H-2, H-6), 7.35−7.55 (m, 12H, H-arom, H-α, H-β), 7.62 (d, 1H, H-6′, ^3J = 8.63 Hz). M + 1 = 465.2.

1-(2,4-Bis-benzyloxy-phenyl)-3-(4-hydroxy-3,5-dimethoxy-phenyl)-propenone (4). Yield 65%, mp 126 °C. ^{1}H NMR (DMSO-d_6, 300 MHz): 3.86 (s, 6H, 2CH$_3$), 5.15 (s, 2H, CH$_2$), 5.23 (s, 2H, CH$_2$), 5.35 (s, 1H, OH), 6.73 (dd, 1H, H-5′ ^3J = 8.67 Hz, ^4J = 2.19 Hz), 6.92 (d, 1H, ^4J = 2.19 Hz, H-3′), 7.25 (s, 2H, H-2, H-6), 7.35−7.55 (m, 12H, H-arom, H-α , H-β), 7.64 (d, 1H, H-6′, ^3J = 8.63 Hz.). M + 1 = 497.3.

3-(4-Hydroxy-3, 5-dimethyl-phenyl)-1-(2-hydroxy-phenyl)-propenone (7). Yield 67%, mp 178−179 °C. ^{1}H NMR ((CD$_3$)$_2$CO, 300 MHz): 2.28 (s, 6H, 2CH$_3$), 6.91−6.97 (m, 2H, H-3′, H-5′), 7.55 (m, 3H, H-2, H-6, H-4′), 7.90 (s, 2H, H-α, H-β), 8.23 (d, 1H, H-6′). M + 1 = 269.2.

1-(4-Benzyloxy-2-hydroxy-phenyl)-3-(4-hydroxy-3,5-dimethyl-phenyl)-propenone (8). Yield 31%, mp 175−176 °C. ^{1}H NMR ((CD$_3$)$_2$CO, 300 MHz): 2.25 (s, 6H, 2CH$_3$), 5.20 (s, 2H, CH2), 6.60 (m, 2H, H-3′, H-5′), 7.45 (m, 7H, H-arom, H-α, H-β), 7.80 (s, 2H, H-2, H-6), 8.15 (d, 1H, H-6′, ^3J = 8.9 Hz). M + 1 = 375.2.

1-(4-Benzyloxy-2-hydroxy-phenyl)-3-(4-hydroxy-3,5-dimeth-oxy-phenyl)-propenone (10). Yield 60%, mp 187 °C. ^{1}H NMR ((CD$_3$)$_2$CO, 300 MHz): 3.85 (s, 6H, 2OCH$_3$), 5.22 (s, 2H, CH$_2$), 5.55 (s, 1H, OH), 6.64 (d, 1H, H-α, ^3J = 15 Hz), 7.20 (s, 2H, H-2, H-6), 7.24−7.48 (m, 5H, H-arom), 7.84(d, 2H, H-4′, ^3J = 7 Hz), 8.3 (d, 1H, H-β, ^3J = 15 Hz), 9.65 (s, 1H, OH). M + 1 = 407.1.

1-(2,4-Dihydroxy-phenyl)-3-(4-hydroxy-3,5-dimethyl-phenyl)-propenone (11). Yield 90%, 215−216 mp °C. ^{1}H NMR ((CD$_3$)$_2$CO, 300 MHz): 2.30 (s, 6H, 2CH$_3$), 6.35 (d, 1H, H-3′, ^4J = 2.4 Hz), 6.45 (dd, 1H, H-5′, ^3J = 8.97 Hz, ^4J = 2.4 Hz), 7.48 (s, 2H, H-2, H-6), 7.85 (s, 2H, H-α, H-β), 7.90 (s, 1H, OH), 8.10 (d, 1H, H-6, ^3J = 8.9 Hz), 9.45 (s, 1H, OH), 10.80 (s, 1H, OH). M + 1 = 285.1.
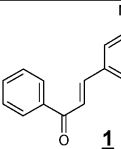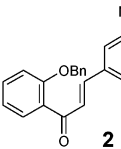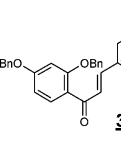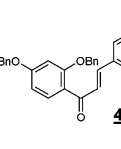
3-(3,5-Di-*tert*-butyl-4-hydroxy-phenyl)-1-(2,4-dihydroxy-phenyl)-propenone (12). Yield 45%, mp 137 °C. ^{1}H NMR (DMSO-d_6, 300 MHz): 1.47 (s, 18H, 2tBu), 3.4 (s, 1H, OH), 6.33(s, 1H, H-6′), 6.49 (d, 1H, H-4′, ^3J = 9 Hz), 7.61 (s, 2H, H-2, H-6), 7.76 (d, 1H, H-α, ^3J = 16.4 Hz), 7.86 (d, 1H, H-β, ^3J = 16.4 Hz), 8.24 (d, 1H, H-3′, ^3J = 6 Hz), 7.59 (d, 1H, H-β, ^3J = 15.87), 7.61 (d, 1H, H-3′). M + 1 = 369.3.

1-(2,4-Dihydroxy-phenyl)-3-(4-hydroxy-3,5-dimethoxy-phenyl)-propenone (13). Yield 41%, mp 218−219 °C. ^{1}H NMR ((CD$_3$)$_2$CO, 300 MHz): 3.90 (s, 6H, 2 OCH$_3$), 6.35 (d, 1H, ^4J = 2.4 Hz), 6.45 (dd, 1H, H-5′, ^3J = 8.8 Hz, ^4J = 2.3 Hz), 7.22 (s, 2H, H-2, H-6), 7.82 (s, 2H, H-α, H-β), 7.90 (1, 1H, OH), 8.10 (d, 1H, ^3J = 8.8 Hz), 9.40 (s, 1H, OH). M + 1 = 317.1

Sensitivity of Molecules to Dioxygen. To avoid degradation by dioxygen, samples were kept after synthesis under argon. No degradation of the neutral samples was observed when sample was exposed to air during 1 day. On the contrary, the corresponding phenolates were found to be sensitive to air and are rapidly oxidized by dioxygen. Neutralization of the polyphenols was always performed after removing O$_2$ by bubbling argon in the solution (see below).

Electrochemistry Experiments. The solvent dimethyl sulfoxide (DMSO) + 0.1 mol L^{-1} NBu$_4$BF$_4$ as supporting electrolyte (Fluka, electrochemical grade) was deoxygenated prior to the dissolution of the compounds. Typical concentrations of polyphenols were in the range of 10^{-3} mol L^{-1} All polyphenols and their corresponding anions were soluble in DMSO at room temperature. The anions of the phenols investigated are highly colored (from raspberry red to carmine and violet). Upon dissolution in DMSO, a light color is often observed, indicating some deprotonation of the phenols; very small waves corresponding to the deprotonated species are observed even in absence of added base. Cyclic voltammetry experiments were performed using a three-electrode setup cell. A Versastat II potentiostat was used together with a homemade potentiostat for higher scan rates.[18] The working electrode was a glassy carbon disk electrode (GC electrode, from Tokai), with a 3 mm diameter for low scan rates or ∼0.2 mm diameter for experiments performed at high scan rates and for the determination of E_p/log(v) plots. They were mechanically polished with 1 μm diamond paste and cleaned with acetone in an ultrasonic bath before each set of voltammograms. The counter electrode was a platinum grid. An aqueous saturated calomel electrode (SCE) was used as a reference. The ferrocene/ferrocenium couple was used as an internal standard for the potential scale taken for the ferrocene/ferrocenium couple $E°$ = +0.405 V versus the SCE and for the determination of the number of electrons involved in the electrochemical reactions. All of the potentials in the text are referenced versus the SCE electrode. Numerical simulations of the voltammograms were performed

TABLE 1: Cyclic Voltammetric Data for Compounds with One OH on Ring A

Compounds with a single OH on Ring A	$E_{pa1}^{a,b}$	$E_{pa2}^{a,b}$	$E_{pa3}^{a,b}$	$E_{pc}^{a,b}$	$E_{paO^-}^{a,b}$ k_{dim}^{c}	$E^{\circ}_{O^-/O\bullet}{}^{b,c}$	$E^{\circ}_{OH/OH\bullet^+}{}^{b}$
1	$+0.85_0$ 1F/mol,Irr[d]	1.14 Irr[d]		-0.19	$+0.15$ >5 10^7	$+0.18$[e]	
2	$+0.82_6$ 1F/mol,Irr[d]	$+1.11$ Irr[d]		-0.35	$+0.10_0$ 10^7	$+0.12$	
3	$+0.79_0$ 1F/mol,Irr[d]	$+1.12$ Irr[d]		-0.39	$+0.06_0$ 3 10^6	$+0.13_1$	
4	$+0.68_2$ 1F/mol,Irr[d]	0.84 Irr[d]		-0.44	-0.04_2 10^6	-0.04	$+0.70$

[a] At 0.2 V s^{-1}. [b] Potentials in volts vs the SCE electrode. [c] Dimerization rate constant calculated for a radical−radical coupling mechanism in L mol^{-1} s^{-1}. [d] Irreversibility at 0.2 V s^{-1}. [e] Estimated from the difference of peak potentials between **1** and **2** and considering a DIM1 mechanism.[26b,c]

with the commercial BAS Digisim Simulator 3.1[19] using the default numerical options with the assumption of planar diffusion.

Electrolyses were performed in a carbon crucible with a platinum counter electrode separated from the cathodic compartment by a glass frit; an Ag/AgCl reference electrode was used. Approximately 25 mg of **1** was dissolved in 10 mL of DMSO + 0.1 mol L^{-1} NBu$_4$BF$_4$, and the potential was set at +0.18 V versus Ag/AgCl, i.e., 50 mV beyond the voltammetric peak of the phenolate. The current decreases very rapidly due to the blocking of the carbon electrode as is very often observed during the oxidation of phenolates. The final solution was diluted with 100 mL of water extracted three times with 50 mL of CH$_2$Cl$_2$ and twice with 50 mL AcOEt; the organic layer was dried and evaporated, and the final traces of remaining DMSO were evaporated with a vacuum pump. Mass spectrum (CI, NH$_3$, M(**1**) = 252): 504 (5, dimer), 399 (18, dimer − C$_6$H$_5$CO), 253 (100, 252 + 1, and 399 − 147, C(=O)CH=CH C$_6$H$_2$ Me$_2$OH−). Compound **2** was electrolyzed in the same way. Mass spectrum (CI, NH$_3$, M(**2**) =358): 717(dimer + 1), 716 (dimer), 585 (717 − CH=CHC$_6$H$_3$Me$_2$), 505 (716 − BnOC$_6$H$_4$C(=O)).

Theoretical Modeling. The calculations were performed using the Gaussian 03W package.[20] Gas-phase geometries and electronic energies were calculated by full optimization without imposed symmetry of the conformations using the B3LYP[21] density functional with the 6-31G* basis set,[22] starting from preliminary optimizations performed with semiempirical methods. We checked that the spin contamination remains low (s^2 < 0.78) for all the open-shell B3LYP calculations. Solvation free energies were calculated on the gas-phase optimized conformations according to the self-consistent reaction field (SCRF) method using the polarizable dielectric method (PCM)[23] and the B3LYP density functional.

Results and Discussion

Cyclic Voltammetry Investigations. The series of hydroxy-chalcones (and polyhydroxychacones) were systematically investigated by cyclic voltammetry, and data were analyzed as function of the number and positions of OH groups to identify their role and interaction. As a first preliminary experiment, the oxidation of the chalcone itself (or 1,3-diphenyl-propenone) containing no OH group on rings A or B, was examined under the experimental conditions used for the other phenolic compounds. Whatever the nature of the electrode, no electrochemical signal corresponding to the oxidation of the molecule was observed before the background discharge, showing that the unsubstituted chalcone cannot be oxidized in DMSO. It is therefore the phenolic functions that undergo oxidation.

Chalcones with One OH on Ring A (1−4). Let us first consider the oxidation of mono-hydroxychalcones, which contain one free phenol group on ring A (Table 1). A typical example of this family is provided by the oxidation of 3,5-dimethyl-4-hydroxychalcone **1** (Figure 1) in DMSO (+0.1 mol L^{-1} NBu$_4$BF$_4$).

The voltammogram shows a first irreversible one-electron oxidation process with a peak potential E_{pa1} located at 0.85 V versus the SCE, followed by a second irreversible process at E_{pa2} = 1.14 V of lower current intensity. On the return scan, a reduction peak appears at E_{pc} = −0.19 V only if the second anodic wave has been scanned beforehand. Upon repetitive scanning, this peak increases and no other peak appears between −0.5 and +1.3 V, indicating that the final oxidation product is reduced at Epc but cannot be further oxidized in that range of potential. The corresponding phenolate was prepared by in situ addition of NMe$_4$OH (half-neutralization).[24]

A new irreversible one-electron oxidation peak appears at E_{paO^-} = 0.156 V versus the SCE, and no cathodic peak can be observed on the return scan down to −0.5 V (Figure 2). This
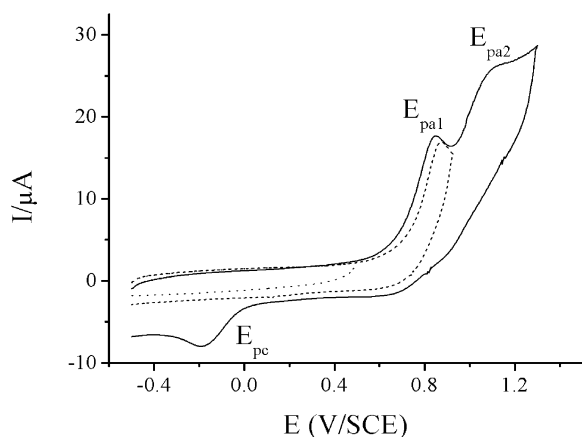
Phenols Deriving from Chalcones

J. Phys. Chem. B, Vol. 109, No. 49, 2005 **23723**

Figure 1. Cyclic voltammetry of **1** (example of chalcone with an OH on ring A) in DMSO + 0.1 mol L^{-1} NBu$_4$BF$_4$. GC electrode. $C = 1.0 \times 10^{-3}$ mol L^{-1}. Scan rate $v = 0.2$ V s^{-1}.
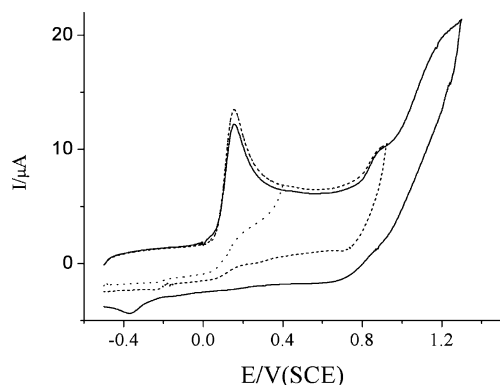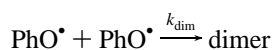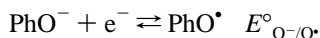

Figure 2. Cyclic voltammetry of **1** in DMSO + 0.1 mol L^{-1} NBu$_4$-BF$_4$. GC electrode. $C = 1.0 \times 10^{-3}$ mol L^{-1} with addition of 5×10^{-4} mol L^{-1} NMe$_4$OH. Scan rate $v = 0.2$ V s^{-1}.

first oxidation is followed by a second one located at the same potential as E_{pa2}; the height of this second peak corresponds to the exchange of one electron per phenolate (taking into account the fact that **1** is only half-neutralized). When the scan rate is increased up to 500 V s^{-1}, no reversibility of the phenolate oxidation is observed, indicating that the lifetime of the electrogenerated phenoxyl radical remains shorter than the experimental time of the cyclic voltammetry (some tenths of milliseconds).

From the shift of the peak potential with the scan rate ($\delta E_{paO^-}/\delta \log(v)$) (Figure 3) and concentration ($\delta E_{paO^-}/\delta \log(c)$), it is possible to determine the order of the reactions following the electron transfer.[25] For **1**, linear variations were found with slope values of 21.0 mV/log(v) and 19 mV/log(c). As seen in Table 1, similar values were obtained for all of the molecules of this family. These data are in agreement with the theoretical slopes predicted for a mechanism involving a fast electron transfer followed by an irreversible dimerization (radical−radical coupling or DIM1 mechanism).[26] On the basis of this analysis, the following mechanism can be proposed involving the coupling between two phenoxyl radicals

$$PhO^- + e^- \rightleftarrows PhO^\bullet \quad E^\circ{}_{O^-/O^\bullet}$$

$$PhO^\bullet + PhO^\bullet \xrightarrow{k_{dim}} dimer$$

Exhaustive electrolysis of phenate **1**$^-$ species was performed in the same conditions (after half-neutralization of **1**) at the level of its first oxidation potential. Analysis of the resulting solution
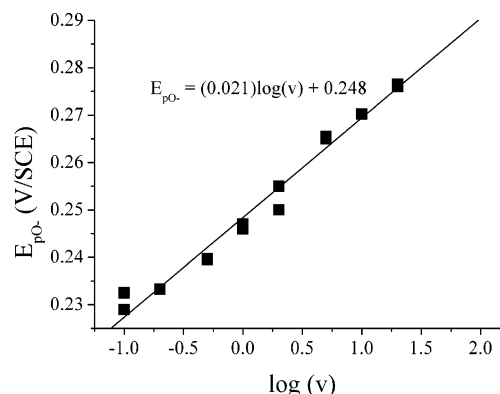

Figure 3. E_{pO^-} vs log(v) for compound **1** in DMSO + 0.1 mol L^{-1} NBu$_4$BF$_4$. GC electrode. $C = 1.0 \times 10^{-3}$ mol L^{-1} with addition of 5×10^{-4} mol L^{-1} NMe$_4$OH. Scan rate $v = 0.2$ V s^{-1}.

by mass spectroscopy reveals the presence of dimer(s) in agreement with the kinetics analysis. Concerning the structures of these dimers, five mesomeric forms can be written for the radical obtained by oxidation of the conjugate system including ring A; therefore a large number of dimers can be formed, and generally many dimers are obtained during the oxidation of phenolates, making the analysis of final mixtures difficult. Besides, because the electrolysis stops quite rapidly due to the fouling of the electrode (probably by these same dimers), the final mixture mainly contains the starting phenolate. However, the observation of a peak at $m/z = 399$ corresponding to the loss of C$_6$H$_5$C=O indicates that the dimerization does not take place on ring B (this is expected from the mesomeric forms and from the density functional theory (DFT) calculations) or on the carbonyl. We are therefore left with 10 possibilities for the structures of the dimers. Among these possibilities quinones should be excluded because the cyclic voltammetry does not indicate the possibility of such compounds, which should appear as reversible systems at about 0 V versus the SCE.

For phenolate **2**$^-$ that contains a benzyloxy group on ring B, the cyclic voltammetry (at 0.2 V s^{-1}) displays the same general pattern as that of **1**$^-$. A linear E_{paO^-}/log(v) plot is observed with a slope $\delta E_{paO^-}/\delta \log(v)$ of 22.5 mV/log(v), which shows the occurrence of similar DIM1 mechanisms for the oxidations of **2**$^-$ and **1**$^-$. As for **1**$^\bullet$, the occurrence of a dimerization in the case of **2**$^\bullet$ was confirmed by an exhaustive electrolysis and analysis of the solution that provides evidence for the formation of dimer(s) (Experimental Section).

When the scan rate is increased above 200 V s^{-1}, the oxidation of the phenolate becomes partially reversible, meaning that the lifetime of the radical turns out to be of the order of the corresponding experimental time. Compound **3** that contains two benzyloxy groups on ring B shows a nearly identical behavior.

Considering the DIM1 mechanism for the phenolate oxidation, the dimerization rate constants can be extracted by comparison of the experimental voltammograms with simulated curves (calculated with the Digisim software, Experimental Section).[19] The method is based on the analysis of the oxidation reversibility (obtained from the ratio between the anodic and cathodic peak currents) versus the scan rate.[25] An increase of the stability of the phenoxyl radical results in a decrease of the scan rate required for observing the reversibility and vice versa. The dimerization rate constants of the phenoxyl radical, k_{dim}, that range between 5×10^6 and 5×10^7 L mol^{-1} s^{-1}, are considerably lower than the kinetic rates measured for classical phenoxyl radicals (see, for example, the dimerization rate of

TABLE 2: Formal Potentials (V vs the SCE) for Vinylic Phenols

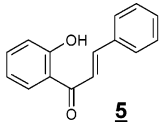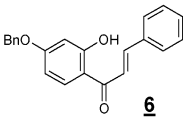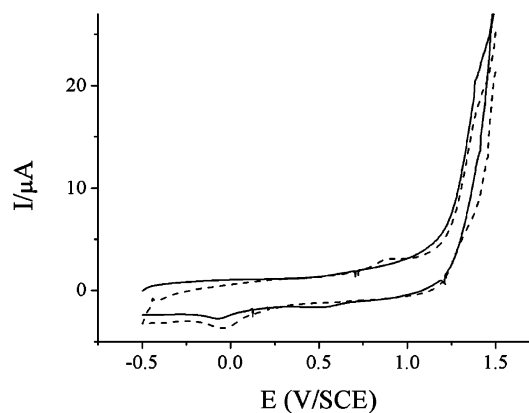|	**2**	coumar-aldehyde	conifer-aldehyde	sinap-aldehyde	**4**
$E°_{O^-/O^\bullet}$	+0.12	$0.64_0{}^a$	$0.47_6{}^a$	$0.30_0{}^a$	−0.04

a From ref 13 in acetonitrile.

the unsubstituted phenoxyl radical itself that was found to be near the diffusion limit).[27]

From the reversible voltammograms, the formal potentials $E°_{O^-/O^\bullet}$ for the phenoxyl radical/phenolate couples can also be derived as the midpoint between the cathodic and anodic peaks (for **2**, $E°_{O^-/O^\bullet} = +0.12$ V).[27] If we compare compounds **1**, **2**, and **3** that carry the same substituents on ring A, then a small but regular decrease of the oxidation potentials E_{pa1} and E_{pa2} and the formal potential $E°_{O^-/O^\bullet}$ are observed in parallel with the introduction of donating substituents on ring B. For example, E_{paO^-} is 100 mV more positive for **1** than for **3**. Simultaneously, the dimerization rate constants decrease from **1** to **3**, indicating a stabilization of the phenoxyl radicals. In compound **4**, when the two methyl groups adjacent to the OH on ring A are changed to methoxy, the morphology of the voltammogram is retained. The different peaks (E_{pa1}, E_{pa2}, E_{pc}, and E_{paO^-}) and the formal potential $E°_{O^-/O^\bullet}$ are shifted to negative potentials by about 90 mV as can be expected from the donating effects of the methoxy groups that modify the energies required for all of the electron transfer steps. This donating stabilization also increases the lifetimes of the electrogenerated radical cation. Indeed, the radical cation formed at the level of the first anodic wave (in experiments performed without neutralization) becomes sufficiently stable to permit the measurement of the standard potential of the phenol/phenoxonium radical cation $E°_{OH/OH^{\bullet+}} = +0.70$ V.[28]

It is also interesting to compare the standard potentials $E°_{O^-/O^\bullet}$ of the compounds in Table 1 with those of coumaraldehyde, coniferaldehyde, and sinapaldehyde[13] (Table 2), which have similar structures but lack the presence of ring B. This ring has a very strong effect as it shifts the formal potentials $E°_{O^-/O^\bullet}$ to less positive values by around 300−500 mV (compare **2** with coumaraldehyde and **4** with sinapaldehyde), indicating the strong donating effect of ring B on the electrochemistry of the conjugated system including ring A. On the contrary, comparison of **1** and **2** shows that further substitution on B (addition of a benzyloxy group on the 2′ position) has a very weak effect (30−40 mV). The substitution by a second benzyloxy group on the 4′ position has a similar effect.

Figure 4. Cyclic voltammetry of **5** (example of chalcone with an OH group on ring B). GC electrode. $C = 1.0 \times 10^{-3}$ mol L^{-1}. Scan rate $v = 0.2$ V s^{-1}. First scan (—), 10th scan (- - -).

Chalcones with One OH on Ring B (5 and 6). The behavior of this second family (Table 3) is illustrated by compounds **5** (Figure 4) and **6**.

Their electrochemical patterns are very different from the previous compounds. A single irreversible bielectronic wave is observed at a positive potential close to the solvent oxidation (around +1.3 V), showing that the oxidation of **5** and **6** is much more difficult than that of the previous chalcones **1−4**. After half-neutralization, a new peak appears at a less positive potential corresponding to the oxidation of the phenolate.
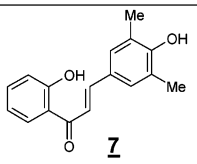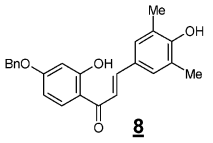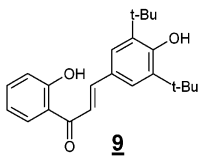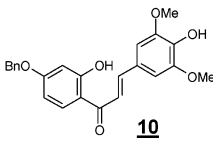
When the scan rate is increased, the reversibility of the phenolate/phenoxyl radical couple could only be observed for **5**. The addition of a bulky (benzylated) OH group on ring B for **6** increases the lifetime of the corresponding radical and makes the scan rate required to observe the reversibility lower for **6** than that for **5**, allowing an estimation of the decay rate constant and the measurement of the formal potential $E°_{O^-/O^\bullet}$. As we noticed for the previous family, the dimerization rate constant was found to be lower than the values measured for "classical" phenoxyl radical. This increase of stability may be ascribed to some steric hindrance in the coupling step.

Chalcones with OH Groups on Rings A and B (7−10). Let us now consider the derivatives bearing one phenol group on each ring A and B (Table 4).

A first glance at Table 4 indicates that the voltammetric patterns of **7** (Figure 5), **8**, **9**, and **10** appear as the addition of the electrochemical features of compounds with OH groups on

TABLE 3: Cyclic Voltammetric Data for Compounds with a Single OH on Ring B

Compounds	$E_{pa1}{}^{a,b}$	$E_{pa2}{}^{a,b}$	$E_{pa3}{}^{b}$	$E_{pc}{}^{a,b}$	$E_{paO^-}{}^{a,b}$ $k_{dim}{}^{e}$	$E°_{O^-/O^\bullet}{}^{b}$	$E°_{OH/OH^{\bullet+}}{}^{b}$
5			~+1.35 2F/mol, Irr^c	−0.07	$+0.41_2$ 5×10^6	~+0.4	
6			$+1.34_8$ 2F/mol, Irr^c	−0.14	$+0.49_6$	d	

a At 0.2 V s^{-1}. *b* Potentials in volts vs the SCE. *c* Irreversible at 0.2 V s^{-1}. *d* $E°$ cannot be measured as the reversibility cannot be observed. *e* Dimerization rate constant of the phenoxyl radical in L mol^{-1} s^{-1}.

Phenols Deriving from Chalcones

J. Phys. Chem. B, Vol. 109, No. 49, 2005 **23725**

TABLE 4: Cyclic Voltammetric Data for Compounds with One OH on Both Rings

Compound	$E_{pa1}^{a,b}$	$E_{pa2}^{a,b}$	$E_{pa3}^{a,b}$	$E_{pc}^{a,b}$	$E_{paO}^{-a,b}$ k_{dim}^{f}	$E°_{O^-/O•}^{b}$	$E°_{OH/OH•^+}^{b}$
7	$+0.84_2$	$+1.08$	$\sim +1.24$	-0.32	$+0.19_0$	$+0.20_1$	
	$1F/mol,Irr^c$	$Irr^{c)}$		$Irr^{c)}$	5×10^6		
8	$+0.78_0$	$+1.07$	$d)$	-0.33	0.14_6	$+0.18$	
	$1F/mol,Irr^c$	Irr^c		Irr^c	3×10^6		
9	$+0.84_0$	$+1.22$	$\sim +1.35$	-0.31	$+0.14_5$	$+0.21$	
	$1F/mol,Irr^c$	Irr^c	Irr^c	Irr^c	3×10^6		
10	$+0.64_2$	$+0.82$	$+1.32$	e	$+0.02_4$	$+0.02$	$+0.67$
	$1F/mol,Irr^c$	Irr^c	Irr^c		1×10^6		

[a] At 0.2 V s^{-1}. [b] Potentials in volts vs the SCE. [c] Irreversible at 0.2 V s^{-1}. [d] Poorly defined. [e] Not observed. [f] Dimerization rate constant in L mol^{-1} s^{-1}.
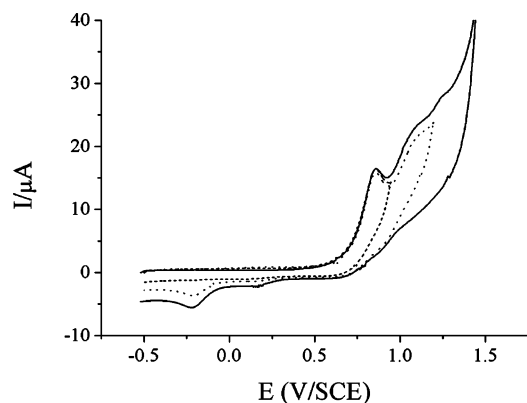

Figure 5. Cyclic voltammetry of **7** (example of chalcone with an OH on ring A and ring A). GC electrode. $C = 1.1 \times 10^{-3}$ mol L^{-1}. Scan rate $v = 0.2$ V s^{-1}.

ring A (Table 1) and those with OH groups on ring B (Table 3).

This can be interpreted in the following way: The first two oxidation steps take place on the conjugated system containing the phenol group on ring A that presents the lowest oxidation potentials (see DFT calculations). This oxidation leads to an intermediate where the structure of ring B remains similar to that of **5** or **6** (Table 3), suggesting that ring B is not directly involved in the first oxidation step. This compound is then oxidized in step 3. The standard potentials $E°_{O^-/O•}$ of the phenolates were measured after half-neutralization and derived from the reversible voltammograms recorded at high scan rates.

The $E°_{O^-/O•}$ values reported in Table 4 are just slightly more positive than those measured for chalcones with OH on ring A and show some small effects of the ring B substitution on the oxidation of ring A. Comparison of **7** and **9** indicates that the
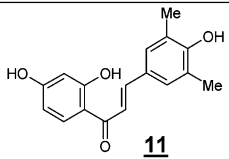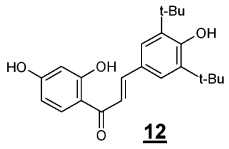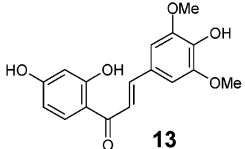
replacement of the 3,5-methyl groups by *tert*-butyl groups has no measurable effect on the redox potentials.

Chalcones with Two OH Groups on Ring A and One on Ring B (11−13). The electrochemical behavior of the neutral molecules **11−13** (Table 5) is very similar to that of the compounds of Table 4.

After half-neutralization, the $E_p/\log(v)$ plots are linear and close to 20 mV/log(v) as found for the other hydroxychalcones. It is noticeable that the presence of an additional OH group on the 4′-position (ring B) does not considerably modify the oxidation patterns of these compounds. Comparison of **7** and **8** provides the effect of a donating a benzyloxy group on the 4′-position; it shifts negative (cathodic) (as expected for a donating group), E_{pa1} by 60 mV and $E°_{O^-/O•}$ by 20 mV. Comparing the standard potential $E°_{O^-/O•}$ between **7** and **11**, one observes a small change of approximately 10 mV, indicating that even with the two OH groups on ring B, ring A is the only oxidized moiety. Addition of an additional hydroxy group on the 4′-position, (compare **7** and **11** as well as **9** and **12**) creates a weak donating effect that translates to a cathodic shift of 30−40 mV for E_{pa1} and at most 40 mV for $E°_{O^-/O•}$. The effect of the 3−5 dimethoxy groups is the same as that already observed, providing a shift of 100 mV for E_{pa1} and of 150 mV for $E°_{O^-/O•}$.

DFT Calculations. To help in the interpretation of the experimental data concerning the electrochemical behavior of hydroxychalcones, we performed quantum chemical calculations based on DFT methods (B3LYP/6-31G* level). The B3LYP method with the 6-31G* base was previously used for similar molecules involving conjugated phenolic compounds and found to provide a good level for the prediction of their electrochemical and chemical properties (spin distribution in the radicals, variation of the oxidation potentials, etc.).[12] The geometries were calculated after a full optimization without constraint starting

TABLE 5: Cyclic Voltammetric Data (V vs the SCE) for Compound with Three OH Groups

Compound	E_{pa1}[a,b]	E_{pa2}[a,b]	E_{pa3}[a,b]	E_{pc}[a,b]	E_{paO-}[a,b] k_{dim}	$E°_{o-/o\cdot}$[b]	$E°_{OH/OH\cdot+}$[b]
11	$+0.81_8$ 1F/mol,Irr[c]	$+0.97$ Irr[c]	$+1.21$ Irr[c]	-0.33	$+0.17_6$ 10^6	$+0.19$	
12	$+0.80_0$ 1F/mol,Irr[c)]	$+1.06$ Irr[c)]	d)	-0.4	$+0.146$ 5×10^6	$+0.17_1$	
13	$+0.70_6$ 1F/mol,Irr[c]	$+0.89$ Irr[c]	$+1.41$ Irr[c]	$+0.14$	$+0.02_8$	$+0.05$	$+0.6$

[a] At 0.2 V s^{-1}. [b] Potentials in volts vs the SCE. [c] Irreversible at 0.2 V s^{-1}. [d] Not observed.
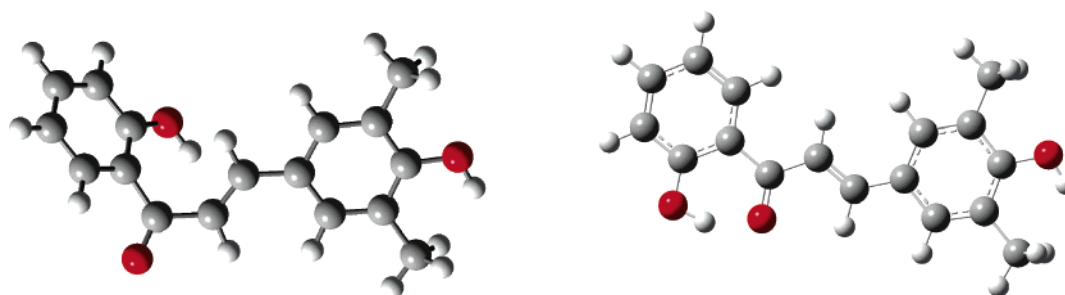

Figure 6. B3LYP/6-31G* optimized geometries for chalcone **7**. Left panel: without hydrogen bonding between O−H on ring B and the C=O. Right panel: with hydrogen bonding.

from a conformation where ring B was prepositioned versus the C=O group. For the neutral chalcones containing one OH on the 2′-position of ring B (**5**, **7**, and **11**), two energy minima were obtained depending on the relative position of the OH versus the carbonyl in the starting geometry. In the first case, a conformation with the O−H pointed to the C=O was obtained, suggesting the existence of hydrogen bonding between the O−H of phenol A and the C=O of the carbonyl (Figure 6, right panel). These hydrogen-bonded conformations were found to be the most stable with stabilization energies around 0.50 eV for **5** and **7** by difference with the corresponding geometries where the OH is far from the C=O.
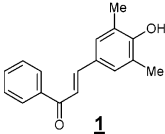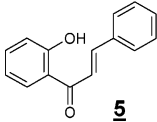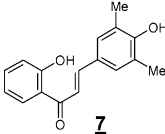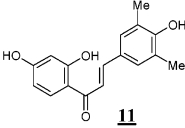
Similar calculations were performed for the radical and anionic species. As seen in Table 6, the radicals and the anions on ring A are the most stable (lower electronic energies) in agreement with the higher delocalization. As an example, Figure 7 displays the optimized geometries and the spin densities on the two possible radicals for chalcone **7**.[29] Besides the larger delocalization for the ring-A-type radical, the spin density is distributed in totally different parts of the molecule, indicating that when the chalcone contains OH groups on both rings A and B the two parts of the molecule should behave almost independently.

In the case of **7** or **11**, we should notice that the hydrogen bonding still exists when the radical or the phenolate anion is formed on ring A. The stabilization energies are not considerably

modified and found to be 0.57 eV in the phenoxyl radical and 0.53 eV in the phenolate (for **11**). This confirms that a low degree of interaction exits between the two phenol rings and thus that the formation of a radical or an anion on ring A has little influence on the properties of ring B. In solution, DMSO molecules can also act as hydrogen bond acceptors[30] and thus will compete with the intramolecular hydrogen bonding discussed here. In previous calculations performed by DFT in the gas phase that maximize the effect, the hydrogen bonding energy between DMSO and phenol was estimated to be around 0.3 eV.[31] If this value is not negligible, then it remains considerably lower than the intramolecular hydrogen bond energy, thus indicating that even in this type of solvent the intramolecular hydrogen bonding still exists.

Other interesting information arises from the DFT electronic energies U_{el} for radicals and anions and their comparisons with the experimental potentials. In a series of hydroxychalcones, the variations of the formal potentials $E°_{O^-/O\cdot}$ can be compared with the differences $\Delta U_{el,ox} = U_{elec(radical)} - U_{elec(anion)}$ (U_{el} for radicals and anions, respectively). Similarly, the variation in the acidity (relative pK_a) can be compared with the differences $\Delta U_{el,acidity} = U_{elec(anion)} - U_{elec(neutral)}$ (U_{el} for anions and neutral, respectively). To limit the influence of systematic errors arising from the method of calculation, we chose to make these comparisons on the same molecule **11** that gathers all the position possibilities and for which we calculated U_{el} for the

TABLE 6: B3LYP/6-31G* Energies (in Hartrees) of Optimized Geometries[a]

Compound	Neutral	Anion A	Anion B	Radical A	Radical B
	without H-bond	without H-bond	without H-bond	without H-bond	without H-bond
	with H-bond	with H-bond	with H-bond	with H-bond	with H-bond
1	-807.888823	-807.349153	-	-807.261288	-
	-	-	-		-
5	-729.250623	-	-728.695174	-	-728.609795
	-729.268952	-	-	-	-
7	-883.105606	-882.572687	-882.546159	-882.476474	-882.464480
	-883.123972	-882.591436	-	-882.495891	-
11	-958.324050	-957.790036	-957.769094	-957.695258	-957.683415
	-958.343815	-957.809441	-957.793940	-957.716165	-957.700004
			Ring B$_{meta}$		*Ring B$_{meta}$*
			-957.766762		-957.682304
			-		-

[a] The meta position denotes the OH radical formation site in reference to the OH engaged in the hydrogen bonding.
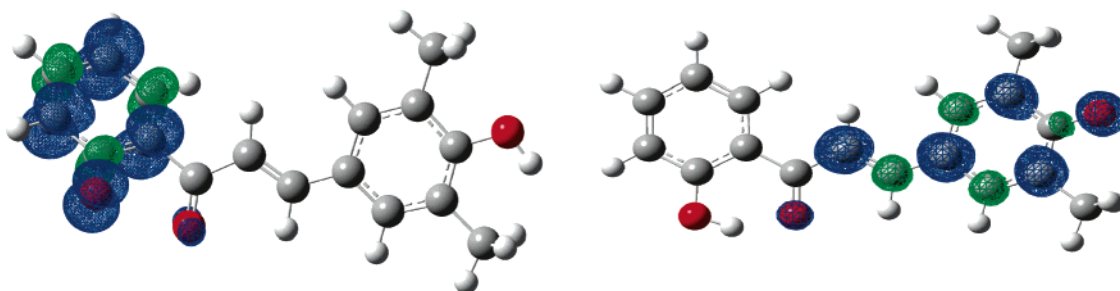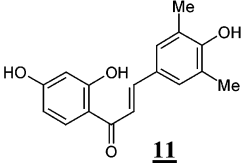

Figure 7. B3LYP/6-31G* optimized geometries for chalcone **7**. Spin densities (0.004 u.a.) for B (left panel) and A (right panel) ring localized radicals.

TABLE 7: Electronic Energies in DMSO (PCM) at the B3LYP/6-31G* Level, Estimations of pK_a and Variations in Formal Potentials

Compound	OH Position	U_{el} Anion[a]	U_{el} Radical[a]	$\Delta U_{el,acidity}$[b]	$\Delta U_{el,ox}$[b]
	Ring B$_{para}$ (4'-OH)	-957.865002	-957.701557	13.35	4.45
11	*Ring B$_{meta}$ (2'-OH)*	-957.854069	-957.697947	13.49	4.29
	Ring A (4-OH)	-957.870197	-957.720856	13.05	4.06

[a] Electronic energies in DMSO (PCM) in hartrees. For the neutral **11** = −958.350126 hartrees. [b] ΔU_{el} relative to acidity (pK_a) and phenolate oxidation ($E°_{O^-/O•}$) in electronvolts.

different possible anions and radicals. To take solvation into account the PCM model[23] was used to estimate the electronic energies in DMSO as a compromise between accuracy and calculation time.

A first glance at Table 6 shows that radical A and phenolate A are clearly the most stable species. The same conclusions are also drawn from the calculated ΔU_{el} differences in Table 7 relative to pK_a and $E°_{O^-/O•}$, indicating that anion A and radical A are the easiest species to be formed (this is most likely related to the bright colors of the conjugated anions). More precisely for the deprotonation, the order was A, B$_{para}$, and B$_{meta}$ (or the 4-OH, 4'-OH, and 2'-OH positions. These deprotonations occur with a large energy variation for the last one because the formation of the phenolate on ring B must break the hydrogen
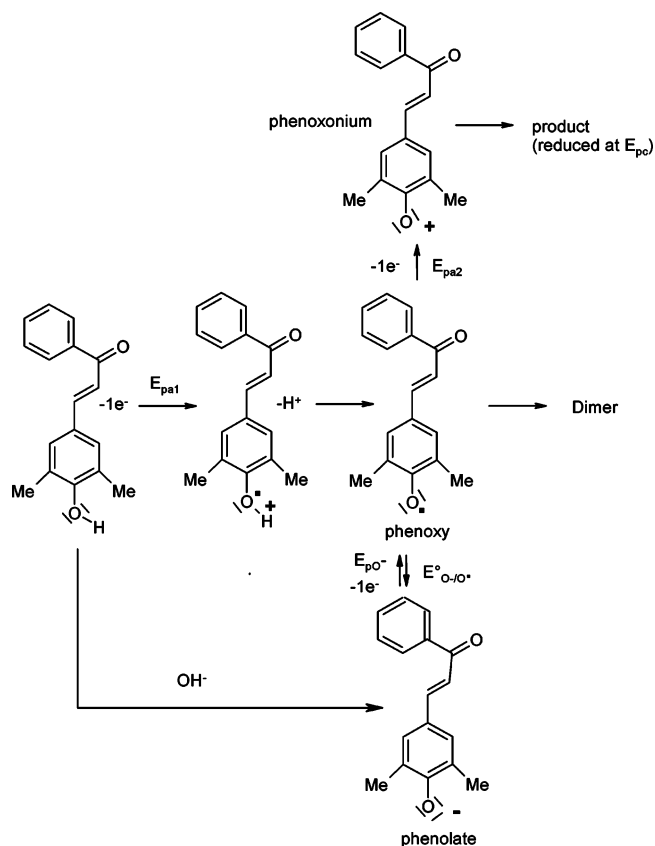
bonding. For the oxidability, the order was A, B_{meta}, and B_{para}, which is clearly more difficult to form than the two other radicals (by around 0.4 eV). In this comparison, we should notice that when the OH is located on the 2′-position (B_{meta}) the hydrogen bond is already broken before the phenolate oxidation.

Hydrogen Bonding Effect. Experimentally, the comparison between Tables 1 and 3 should reflect the effects of the presence of the hydrogen bond. In the DFT calculations, we found that upon oxidation of the phenolate to the phenoxyl radical the hydrogen bond between the hydroxyl groups of ring B and the carbonyl is not considerably affected. Therefore, the difference $E°_{O^-/O^•}(\mathbf{2}) - E°_{O^-/O^•}(\mathbf{7}) = 0.12 - 0.20 = -0.08$ V provides an experimental view of the variation of the hydrogen bonding energies between the phenolate and the phenoxyl radical because the intramolecular hydrogen bond does not exist in **2**. The DFT calculations in the gas phase predict similar small variations around -0.05 eV.[32] This means that if the individual effects of the hydrogen bonding in the phenol, the phenoxyl radical, or the phenolate are strong (stabilization energies by hydrogen bonding around 0.5 eV), then they compensate in the $E°$ values, which are not considerably influenced by the hydrogen bonding. In the same way, the difference of $E°_{O^-/O}$ between **4** and **10** gives an energy in the same range of 0.04 eV, thus confirming that the hydrogen bonding is not broken by the oxidation. The comparison of the oxidations of the neutral phenols **1**, **2**, and **7** shows negligible differences (<20 mV), which also indicates that the hydrogen bond is not broken at the level of the radical cation. Even if the existence of intramolecular hydrogen bonding does not considerably modify the oxidation potentials, the hydrogen bonding should affect the rigidity and the geometry of the ring B$-\alpha,\beta$-ethylenic ketone system, because ring B cannot freely rotate without breaking the hydrogen bond linkage. This constrained geometry should strongly influence the interaction of these systems with biological sites, for example, the active sites of enzymes.

Oxidation Mechanism. From the above results, in the neutral hydroxychalcones bearing an OH group on ring A, the first electron transfer leads to a radical cation that deprotonates to a phenoxyl radical only localized on ring A, as confirmed by the DFT calculations. This radical is then oxidized to a phenoxonium cation on the second one-electron transfer. This cation leads to a product that is easily reduced at low cathodic potentials E_{pc} on the reverse scan. In basic DMSO, the produced phenolates are much easier to oxidize than the corresponding phenols (oxidation in the 0−0.2 V vs the SCE range). The first one-electron wave (E_{paO^-}), followed at a more positive potential by a second one-electron process, is located exactly at the same potential as the second peak of the phenol itself E_{pa2}. This confirms that the second wave of the phenol at E_{pa2} corresponds indeed to the oxidation of the phenoxyl radical to its phenoxonium ion and thus that the same phenoxyl radical is formed in neutral and basic media. The values of $\delta E_{paO^-}/\delta\log(\nu)$ and $\delta E_{paO^-}/\delta\log(c)$ of approximately 20 mV/log(ν) or -20 mV/log-(c) indicate that the first electron transfer is fast and followed by a second-order homogeneous reaction (the coupling between two radicals), which leads to a dimer. The formation of this dimer is confirmed by the mass spectroscopic analysis of the electrolysis products. In agreement with the voltammetric observations in neutral and basic DMSO, we can summarize the mechanisms as in Scheme 1 (exemplified for **1**).

The oxidation patterns for the two compounds that present a single free hydroxyl group on ring B are quite different (Table 3 for **5** and **6**). A single two-electron wave is observed for the phenol oxidation at more positive potentials (around 500 mV),[33]

SCHEME 1

and the structure of the generated product is very different because its reduction takes place 300 mV less cathodic. Concerning the oxidation of the corresponding phenolates (**5⁻** and **6⁻**), their oxidation is also more difficult in agreement with a lesser conjugation of ring B. As is visible from spin densities calculated by DFT, the delocalization of the unpaired electron is limited to ring B in contrast to the other radical where the unpaired electron spreads over the conjugated system. Estimations of the oxidation potentials by DFT confirm that the phenoxyl radical on ring A is more stable than the one on ring B (Table 7). The phenoxyl radical from **6** displays a decay rate k_{dim} in the same range as the other radicals of Table 1. Concerning the phenolate, it is also noticeable that phenolate/phenoxyl couples localized on ring B display broader voltammograms than those centered on ring A. This observation can be ascribed to a slower electron transfer when ring B is involved, which strongly suggests that the charge of the anion centered on ring B is more localized than for those centered on ring A.[25,34]

The third family contains the compounds **7**−**10** (Table 4) bearing a free hydroxyl group on both rings A and B. The oxidation scheme of the neutral phenol appears as the sum of the oxidation features of compounds containing a single OH on ring B and those with a single OH on ring A.[35] This is confirmed by DFT calculations, which indicate as shown in Figure 7 the existence of two independent radicals where the spin density does not delocalize from one system to the other. The oxidation patterns of the corresponding phenolates are different from those of the neutral forms; one observes a single oxidation wave at E_{pO^-} located at potentials very close to those of Table 1 (only slightly positive 60−80 mV), indicating again that the electron transfer principally involves ring A in agreement with the spin repartition calculated by DFT.

For all of these molecules the radical phenoxyl of chalcone is more stable than the simple phenoxyl radical (for example,

Phenols Deriving from Chalcones

J. Phys. Chem. B, Vol. 109, No. 49, 2005 **23729**

as compared with the radical produced by oxidation of the unsubstituted phenol)[27] because the dimerization rate constants, k_{dim}, that range between 5×10^6 and 5×10^7 L mol^{-1} s^{-1} are much below the diffusion rate limit. This lower reactivity can be explained by the large delocalization of radical A on the α,β-ethylenic ketone system or by some steric hindrance when the 2'-OH position of ring B is involved in the oxidation (hydroxychalcones with an OH group on ring B only).

Conclusion

The electrochemistry of these polyphenols is clearly dominated by the conjugated system phenolic ring A–double bond–ketone, which is the most easily oxidized (if the phenol group remains protonated) or the only one to be oxidized if the phenolic group is deprotonated. However, the oxidation of this conjugated system is strongly influenced by the presence of ring B and to a lower extent by the substituents present on ring A. It is noticeable that the oxidation on ring A is thermodynamically and also kinetically favored because the electron transfer is intrinsically faster for ring A due to the delocalization of the charge on the vinylic system. Oxidation potentials of the phenolates are found to be in the 0.1–0.2 V versus the SCE range that correspond to species that are very easy to oxidize and lead to the rapid formation of nonradical species, underlining the potential antioxidant properties of these molecules. When an OH group is present on ring B, an important feature is the existence of strong hydrogen bonding that remains even when ring A is oxidized or the phenol is deprotonated. The hydrogen bonding does not modify the redox or directly the antioxidant power but considerably increases the rigidity of the molecules that remain planar in the neutral, anionic, and radical forms. From the data gathered in this paper and the above interpretations, it should be possible to predict quantitatively the expected antioxidant properties of natural and new synthetic hydroxy-chalcones.

References and Notes

(1) Star, A. E.; Mabry, T. J. *Phytochemistry* **1971**, *10*, 2812.

(2) Stevens, J. F.; Taylor, A. W.; Nickerson, G. B.; Ivancic, M.; Henning, J.; Haunold, A.; Deinzer, M. L. *Phytochemistry* **2000**, *53*, 759.

(3) Satyanarayana, K.; Rao, M. N. A. *Indian Drugs* **1993**, *30*, 313.

(4) Shibata, S. *Stem Cells* **1994**, *12*, 44.

(5) Dhar, D. N. *The Chemistry of Chalcones and Related Compounds*; Wiley: New York, 1981

(6) Ruby, J. A.; Sukumaran, K.; Kuttan, G.; Rao, M. N. A.; Subbaraju, V.; Kuttan, R. *Cancer Lett.* **1995**, *97*, 33.

(7) Maggiolini, M.; Statti, G.; Vivacqua, A.; Gabriele, S.; Rago, V.; Loizzo, M.; Menichini, F.; Amdo, S. *J. Steroid Biochem. Mol. Biol.* **2002**, *82*, 315.

(8) Tamir, S.; Eizenberg, M.; Somjen, D.; Izrael, S.; Vaya, J. *J. Steroid Biochem. Mol. Biol.* **2001**, *78*, 291.

(9) (a) Lebeau, J.; Furman, C.; Bernier, J. L.; Duriez, P.; Teissier, E.; Cotelle, N. *Free Radical Biol. Med.* **2000**, *29*, 900. (b) Furman, C.; Lebeau, J.; Fruchart, J.; Bernier, J.; Duriez, P.; Cotelle, N.; Teissier, E. *J. Biochem. Mol. Toxicol.* **2001**, *15*, 270.

(10) Lebeau, J.; Neviere, R.; Cotelle, N. *Bioorg. Med. Chem. Lett.* **2001**, *11*, 23.

(11) (a) Kashima, M. *Chem. Pharm. Bull.* **1999**, *47*, 279. (b) Hanasaki, Y.; Ogawa S.; Fukui, S. *Free Radical Biol. Med.* **1994**, *16*, 845. (c) Salah, N.; Miller, N. J.; Paganga, G.; Tijburg, L.; Bolwell, G. P.; Rice-Evans, C. *Arch. Biochem. Biophys.* **1995**, *322*, 339. (d) Rice-Evans, C. *Biochem. Soc. Symp.* **1994**, *61*, 103. (e) Vinson, J. A.; Hontz, B. A. *J. Agric. Food Chem.* **1995**, *43*, 401. (f) Nakao, M.; Takio, S.; Ono, K. *Phytochemistry* **1998**, *49*, 2379.

(12) Cren-Olivé, C.; Hapiot, P.; Pinson, J.; Rolando, C. *J. Am. Chem. Soc.* **2002**, *124*, 14027.

(13) Hapiot, P.; Pinson, J.; Francesh, C.; Mhamdi, F.; Rolando, C.; Neta, P. *J. Phys. Chem.* **1994**, *98*, 2641.

(14) Fulcrand, H.; Hapiot, P.; Neta, P.; Pinson, J.; Rolando, C. *Analusis* **1997**, *25*, M38.

(15) Wittman, H.; Uragg, H. *Monatsh. Chem.* **1967**, *98*, 404.

(16) Lmafuku, K.; Honda, M.; McOmie, J. F. W. *Synthesis* **1987**, *2*, 199.

(17) Jain, A. C.; Mehta, A. *Tetrahedron* **1985**, *41*, 5933.

(18) Garreau, D.; Savéant, J.-M. *J. Electroanal. Chem.* **1972**, *35*, 309.

(19) Rudolph, M.; Reddy, D. P.; Feldberg, S. W. *Anal. Chem.* **1994**, *66*, 589A.

(20) Frisch, M. J.; Trucks, G. W.; Schlegel, H. B.; Scuseria, G. E.; Robb, M. A.; Cheeseman, J. R.; Montgomery, J. A., Jr.; Vreven, T.; Kudin, K. N.; Burant, J. C.; Millam, J. M.; Iyengar, S. S.; Tomasi, J.; Barone, V.; Mennucci, B.; Cossi, M.; Scalmani, G.; Rega, N.; Petersson, G. A.; Nakatsuji, H.; Hada, M.; Ehara, M.; Toyota, K.; Fukuda, R.; Hasegawa, J.; Ishida, M.; Nakajima, T.; Honda, Y.; Kitao, O.; Nakai, H.; Klene, M.; Li, X.; Knox, J. E.; Hratchian, H. P.; Cross, J. B.; Bakken, V.; Adamo, C.; Jaramillo, J.; Gomperts, R.; Stratmann, R. E.; Yazyev, O.; Austin, A. J.; Cammi, R.; Pomelli, C.; Ochterski, J. W.; Ayala, P. Y.; Morokuma, K.; Voth, G. A.; Salvador, P.; Dannenberg, J. J.; Zakrzewski, V. G.; Dapprich, S.; Daniels, A. D.; Strain, M. C.; Farkas, O.; Malick, D. K.; Rabuck, A. D.; Raghavachari, K.; Foresman, J. B.; Ortiz, J. V.; Cui, Q.; Baboul, A. G.; Clifford, S.; Cioslowski, J.; Stefanov, B. B.; Liu, G.; Liashenko, A.; Piskorz, P.; Komaromi, I.; Martin, R. L.; Fox, D. J.; Keith, T.; Al-Laham, M. A.; Peng, C. Y.; Nanayakkara, A.; Challacombe, M.; Gill, P. M. W.; Johnson, B.; Chen, W.; Wong, M. W.; Gonzalez, C.; Pople, J. A. *Gaussian 03*, revision B.04; Gaussian, Inc.: Wallingford, CT, 2004.

(21) Becke, A. D. *J. Chem. Phys.* **1993**, *98*, 5648.

(22) Hariharan, P. C.; Pople, J. A. *Chem. Phys. Lett.* **1972**, *16*, 217.

(23) (a) Cossi, M.; Barone, V.; Cammi, R.; Tomasi, J. *Chem. Phys. Lett.* **1996**, *255*, 327 (b) For a general review about solvation methods see: Cramer, J.; Truhlar, D. G. *Chem. Rev.* **1999**, *99*, 2161.

(24) This procedure was chosen to reduce the degradation of the phenolates that are sensitive to dioxygen. Half-neutralization ensures that only one OH group is neutralized in the case of polyhydroxychalcones with similar pK_a values.

(25) (a) Andrieux, C. P.; Savéant, J. M. In *Investigations of Rates and Mechanisms of Reactions*; Bernasconi, C. F., Ed.; John Wiley and Sons: New York, 1986; Vol. 6, Part 2, pp 305–390. (b) Bard, A. J.; Faulkner, L. R. *Electrochemical Methods: Fundamentals and Applications*, 2nd ed.; John Wiley and Sons: New York, 2000.

(26) (a) Theoretical slopes of $\delta E_p/\delta\log(v) = -19.8$ mV/log(v) and $\delta E_p/\delta\log(c) = 19.8$ mV/log(c) at 25 °C are expected for a DIM1 mechanism.[26b] (b) Nadjo, L.; Savéant, J. M. *J. Electroanal. Chem.* **1973**, *48*, 113. (c) Andrieux, C. P.; Nadjo, L.; Savéant, J.-M. *J. Electroanal. Chem.* **1973**, *42*, 223. (d) Richards, J. A.; Whitson, P. E.; Evans, D. H. *J. Electroanal. Chem.* **1975**, *63*, 311.

(27) Hapiot, P.; Pinson, J.; Yousfi, N. *New J. Chem.* **1992**, *16*, 877.

(28) Some reversibility of the first anodic peak can be observed in the experimental time range accessible in our cyclic voltammetry experiment for scan rates higher than 200 V s^{-1}.

(29) Due to its lower energy, only the radical localized on ring A is experimentally produced.

(30) (a) Bordwell F. G.; McCallum, R. J.; Olmstead, W. N. *J. Org. Chem.* **1984**, *49*, 1424. (b) Bausch, M. J.; Gostowski, R.; Guadalupe-Fasano, C.; Selmarten, D.; Vaughn, A.; Wang, L.-H. *J. Org. Chem.* **1991**, *56*, 7192.

(31) Fu, Y.; Liu, R., Liu, L.; Guo, Q.-X. *J. Phys. Org. Chem.* **2004**, *17*, 282.

(32) From the differences of the quantities ($U_{elec(radical)} - U_{elec(anion)}$) calculated with and without hydrogen bonds with the data of Table 5.

(33) Detailed investigations of this bielectronic process are difficult due to the proximity of the solvent oxidation. It is likely that the single two-electron wave corresponds to the formation of the phenoxonium ion (formation of **5**$^{\bullet+}$ followed by rapid deprotonation then a second irreversible oxidation).

(34) (a) In the framework of the Marcus−Hush model related to electron-transfer dynamics,[34b−f] slower kinetics and thus larger activation energies are related to larger solvation changes accompanying the electron transfer and are generally observed when the charge is localized. (b) Marcus, R. A. *J. Chem. Phys.* **1956**, *24*, 966. (c) Marcus, R. A. *J. Chem. Phys.* **1956**, *24*, 979. (d) Hush, N. S. *J. Chem. Phys.* **1958**, *28*, 962. (e) Hush, N. S. *Trans. Faraday Soc.* **1961**, *57*, 557. (f) Marcus, R. A. J. *Chem. Phys.* **1965**, *43*, 679.

(35) One can observe two oxidation waves E_{pa1} and E_{pa2} located at potentials close to those of Table 1 and a third oxidation wave close to those of E_{pa3} of Table 2. This behavior confirms that the two rings are independent (nonconjugated) and are oxidized separately, the more easily oxidized phenol of ring A being oxidized first followed by the phenol of ring B.